The interaction of local anesthetics with lipid membranes

Patricio A. Zapata-Morin, F.J. Sierra-Valdez, J.C. Ruiz-Suárez *

CINVESTAV-Monterrey, PIIT, Nuevo León 66600, Mexico

ABSTRACT

Molecular Dynamic Simulations are performed to evaluate the interaction of lidocaine, procaine and tetracaine with a lipid membrane. The main interest is to evaluate the structural changes produced by these local anesthetics in the bilayers. Penetration trajectories, interaction energies, entropy changes and an order parameter are calculated to quantify the destabilization of the lipid configurations. We show that such structural parameters give important information to understand how anesthetic agents influence the structure of plasma membranes. Graphic processing units (GPUs) are used in our simulations.

© 2014 Elsevier Inc. All rights reserved.

1. Introduction

Anesthetics are drugs that block the nervous impulse causing temporal disruption of sensation in specific parts of the body [1–3]. Although there are several theories to explain their action, there is a still an unfinished debate. The main approach suggests the existence of specific binding sites on the ion channels that regulate the membrane hyperpolarization [4–10]. Yet, important concerns remain due to the fact that this approach does not take into consideration how anesthetic molecules affect the properties of the lipids surrounding such interaction sites [11–15]. A theory that addresses the anesthetic effect in a more general fashion is based on the old work of Meyer and Overton [16,17]. Succinctly, it teaches us that the oil/water partition coefficient can be seen as a measure of the anesthetic potency: if the drug is soluble in oil, it diffuses into the hydrophobic region of the membrane. The nature of this interaction is non-polar, where van der Waals forces are present [18]. This phenomenon is reduced into a constant induction of dipoles of both anesthetic and the hydrophobic region of the bilayer (hydrocarbonated tails), causing, in general, a destabilization and an increase of the membrane fluidity [19]. Indeed, there are recent studies that demonstrate explicitly [20] and implicitly [21,22], the importance of the polarizability in the drug–lipid interaction. Related to such findings, other researchers have reported that in order to produce anesthesia, local anesthetics must have a large affinity to water [23].

Though local and general anesthetics have different sites of action, they share the same type of electrostatic interaction in proteins or lipids: mostly van der Waals. An exquisite survey about how inhaled anesthetics work has been furnished by Eckenhoff [24]. The author observes that the mechanism of drug action is poorly represented in the pharmacology literature, which remains entrenched in the single-target model for drugs. He proposes, instead, that anesthesia is due to small effects at many biological sites. Though his small-effects-at-many-sites model may be considered inelegant (because it will be difficult to validate) he affirms that this multiple target hypothesis is most consistent with clinical observation, the available data, and the remarkable resistance that this 160 year-old dilemma has offered to solution. Motivated by such rationale, Molecular Dynamic Simulations have been carried out to investigate the molecular mechanism of drug attachment in membranes [25] or in protein cavities [26].

The lipid-centered mechanism cannot be fully discarded in the light of a recent work proposed by Heimburg and Jackson [27,28]. The authors suggest that a mechanical perturbation, a soliton, accompanies the electrical impulse. Looking neural excitability through this novel prism, it is a tantalizing idea to consider local anesthesia as a simple blockage of such putative soliton (the strength of it depends on the compressibility of the medium through which it travels, so if the medium is fluidized the solitary wave weakens). If this interesting idea is right, we need to know how anesthetics cause membrane disruption and therefore fluidization.

Local anesthetics are amphiphilic (i.e. they have polar and non-polar regions) and, clinically, the most commonly used are of the amide-type. However, although they have a polar region,

* Corresponding author. Tel.: +52 8111561740.
  E-mail addresses: jcrs.mty@gmail.com, cruiz@cinvestav.mx (J.C. Ruiz-Suárez).

anesthetics exhibit oil/water partition coefficients larger than one [29] and therefore are prone to interact with the hydrophobic region of the lipid membrane. We use Molecular Dynamic Simulations (MDS) to explore how the structural details of a lipid membrane changes during the interaction of three cationic amphiphilic anesthetic drugs. Needless to say that MDS is a well established tool to study the thermodynamic properties of pure lipid [30–35], and doped [36–39] membranes.

In this work we study the effects of lidocaine ($C_-14H_{22}N_2O$), procaine ($C_{13}H_{20}N_2O_2$), and tetracaine ($C_{15}H_{24}N_2O_2$) on a DPPC ($C_{40}H_{80}NO_8P$) bilayer membrane. For the first time, interaction energies (Coulomb and Lennard-Jones), configurational entropies and order parameters are calculated all together in order to understand the effect of anesthetic drugs on the membrane structure.

2. Methods

2.1. Molecular Dynamic Simulations

Since choline phospholipids are the most abundant species in plasma membranes [40], the membrane we study is formed by 1,2-dipalmitoyl-sn-glycero-3-phosphocholine (DPPC) lipids. 193 of them were grouped in a $10\,nm \times 9\,nm \times 10\,nm$ box to form a bilayer. The superficial extension of the membrane corresponds to the XY plane while Z represents the height. 10 molecules of each drug were studied separately; homogeneously positioned 2 nm above the membrane, at time zero. The 3D structures, force fields, and partial charges of the molecules, were obtained from the following sources: DPPC was obtained from Krüeger and Fischer [41], lidocaine from Högberg et al. [42], procaine and tetracaine were built using the online server PRODRG (available at http://davapc1.bioch.dundee.ac.uk/prodrg/) and swissParam (http://swissparam.ch/) following the indications of diverse references [43–46]. The parameters of the GROMOS 53a6 force field library were used to obtain the information of bonds, dihedral angles and the Lennard-Jones interactions (for more information see Oostenbrink [47]). Once we have the structures and their parameters, the minimum energy states for the drug molecules, prior to the build-up of the systems, are found.

After obtaining the initial output of the system, 15,151 single point charge (SPC) water molecules were added to cover the entire simulation space. 153 of these were substituted by NaCl to emulate a physiological ionic concentration of 0.14 M. A pertinent observation is needed: the drugs studied here are normally (clinically) administrated in a substance with low pH (pH 4–5). Since the pK's of the drugs are around 8, they enter the organism in a protonated state. In this work, the pH of the medium was 7, so they are also protonated.

As a previous step to the MDS, the solvated systems were put through short minimization runs to reach values of 1×10^3 kJ/mol. The parameters employed for the dynamics were as follows: PME (Particle Mesh Ewald) conditions were employed to calculate the electrostatic interaction, then a cut-off of 1.2 nm was assigned to Lennard-Jones and Coulomb interactions. A leap-frog algorithm was employed with time steps of 2 fs. The overall system center of mass translation and rotation was removed at every step. The bond lengths were constrained using the LINCS algorithm [48] with a relative geometric tolerance of 10^{-4}. The system was kept at 37 °C and of 1 bar of pressure. The thermostat we used was the Nose–Hoover [49] and the barostat is based on the work of Parrinello–Rahman [50]. Since earlier work has shown that simulations of membranes and small solutes can been drastically underestimated due to the presence of hidden sampling barriers involving the slow reorganization of the lipid–water interface in response to solute insertion [51,52], we run our MD simulations up to 100 ns with 100 ns to
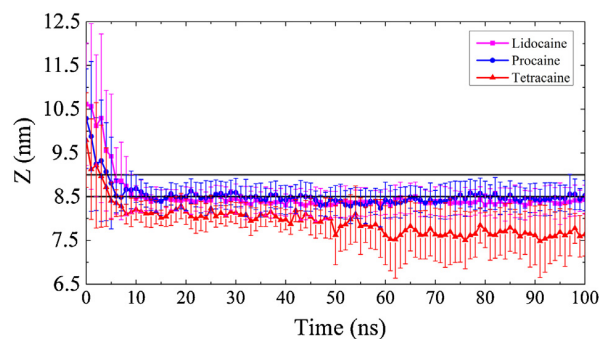

Fig. 1. The distances from the center of the bilayer to the center of mass of a drug, as a function of time. Lidocaine (squares); procaine (circles); tetracaine (triangles). The black lines identify the upper polar region of the membrane, and the center of the bilayer is at $Z = 7$ nm.

pre-equilibrate the system. It is worthwhile to sate here that similar or lesser time lengths are used in related articles [44,45]. We used the GROMACS v.4.6.3 simulation package [53] which run in a GPUs platform. The entire time periods were used for analysis.

It was possible to reduce the degrees of freedom of the system applying the united atom models methodology, following the indications of various articles [37,42,44]. By adding 10 drug molecules (which correspond to a normal dose in anesthesia: around 20 mM) with different initial angles and positions, we avoid the requirement of repeating the simulation a number of times. Then, averaged results are gathered and presented. All simulated drugs reach their final position at around 30–50 ns. The main objective of this article is to differentiate the perturbation each drug causes on the membrane, rather than the time it takes to the system to reach its final equilibrium.

We employed the data obtained from the corresponding Coulomb and Lennard-Jones energies of the 193 lipids that form the membrane interacting with each one of the 10 molecules. In total, we register 3860 interactions per case during the last 80 ns of
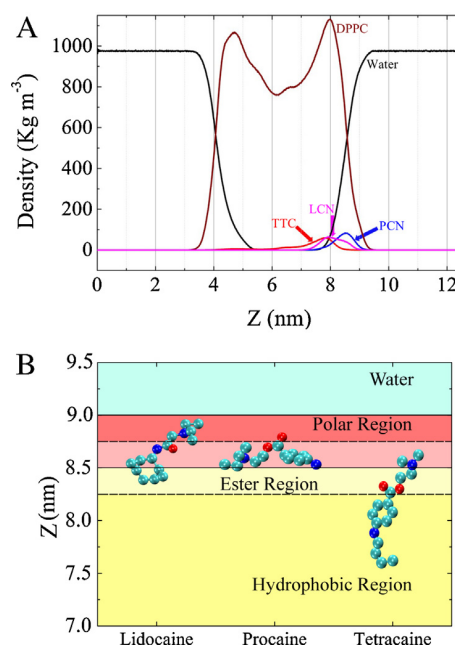

Fig. 2. (A) Mass density profiles for water, lipids, lidocaine, procaine, and tetracaine. (B) Schematic final positions of each drug to illustrate their final orientation. The background shows different regions of the upper lipid bilayer. The center of the bilayer is at $Z = 7$ nm.

Table 1
Summary results of the MD (statistical errors in the parenthesis). γ is the ratio between Lennard-Jones and Coulomb energies.

	DPPC	LCN	PCN	TTC
Coulomb (kJ/mol)		−8.88 (3.55)	−15.56 (7.10)	−10.87 (4.68)
Lennard-Jones (kJ/mol)		−34.12 (8.12)	−27.62 (4.86)	−30.78 (6.73)
γ		3.84	1.77	2.84
Distance to the bilayer center (nm)		1.83 (0.03)	1.87 (0.04)	1.47 (0.05)
Configurational entropies Schlitter (kJ/kmol)	20.64	22.64	22.67	23.09
Freely rotating bonds		5	8	9

the simulation. This allowed us to identify the predominant energy once the molecules reach equilibrium. The center of mass of each drug molecule was tracked with respect to the center of the membrane, on the Z axis of the simulated space, in order to correlate the maximum and minimum energies at their preferential locations.

2.2. Configurational entropy

Any structural change observed in a molecular system can be studied by evaluating its configurational entropy. The quantity depends strongly on the phase space of the system. Schlitter introduced an expression for such entropy based on a quantum-mechanical harmonic approximation [54]. He proposes to use an upper limit given by:

$$S_{true} < S = \frac{K_B}{2} \ln \det \left[1 + \frac{K_B T e^2}{\hbar^2} D \right], \tag{1}$$

where K_B is the Boltzmann's constant, T the absolute temperature, e Euler's number, and $\hbar$ is the Plank's constant divided by 2π. Here, D is the covariance matrix of mass-weighted atomic Cartesian coordinates, defined as:

$$D = \left\langle [M^{1/2}(r - \langle r \rangle)] \otimes [M^{1/2}(r - \langle r \rangle)] \right\rangle, \tag{2}$$

where r is the 3N-dimensional Cartesian coordinate vector of the N particles considered for the entropy calculation after least-squares fitting onto a reference structure, M is the 3N-dimensional diagonal matrix containing the masses of these particles, broken brackets

denote ensemble averaging, and the notation $a \otimes b$ stands for the matrix with elements μ, ν equal to $a_\mu * b_\nu$.

We remove the translation and rotation motion, around the center of mass of the molecule, by performing least-squares fitting of the trajectory configurations of the molecule during the calculation of the covariance matrix. In this form, the translational entropy can be excluded from the calculation but rotational entropy cannot be rigorously separated from internal motion for a flexible molecule [55]. Then, a well approximation of the entropy contributions of internal degrees of freedom (e.g., torsional angles) can be obtained using Cartesian coordinates in the Schlitter's formula.

2.3. Order parameters

We calculate the orientational order parameter S_{CD}. S_{CD} provides information about how well a molecule, o part of a molecule, lines up with a given vector. The order parameter is described as:

$$S^{i+1} = \frac{1}{2} \langle 3\cos^2 \theta^{i+1} - 1 \rangle \tag{3}$$

where θ^{i+1} is the angle between the z-axis of the simulation box and the line that join the carbon atom i with $i+1$. The brackets imply averaging over time and molecules. Order parameters can vary between 1 (full order along the interface normal) and zero in the case of an isotropic orientation.
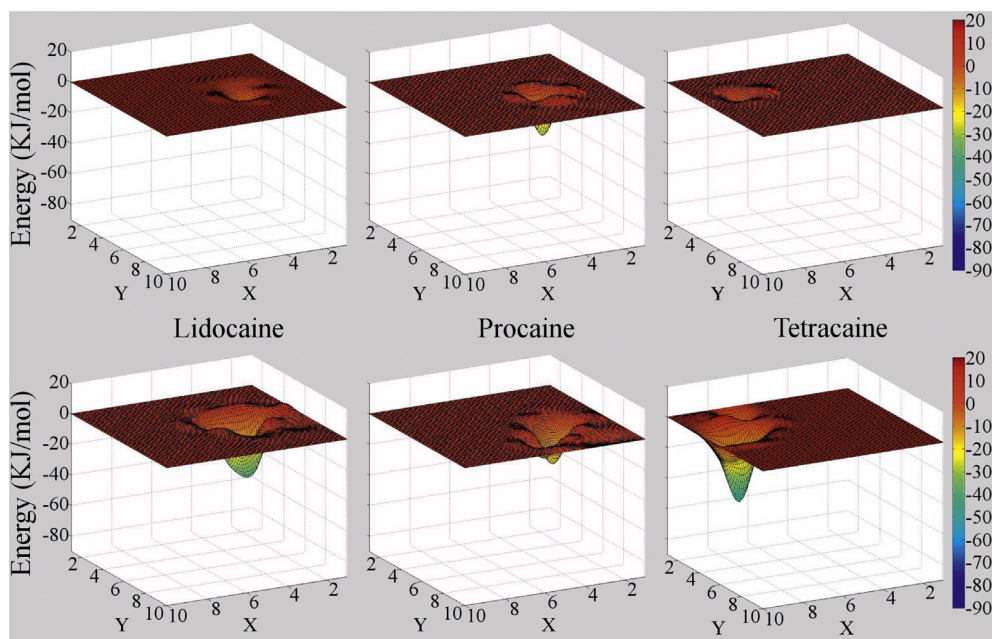

Fig. 3. Snapshots of representative energy profiles. These are constructed by calculating the interaction of each drug, at some given time, with each lipid of the upper membrane surface (an array of 10×10 lipids). Each profile shows the morphology of both the Coulomb (upper graphs) and Lennard-Jones (lower graphs) potentials. The scales in the X–Y planes are in lipid units (~0.8 nm).

3. Results and discussion

3.1. Molecule localization

The trajectories of the drugs as they interact with the membrane are shown in Fig. 1. As we can see, the three drugs insert in the membrane with different degrees of penetration. Lidocaine and procaine insert in the intermediate region (between the hydrated and dehydrated regions), while the last one (tetracaine) is able to reach the alkane core (Fig. 2B). Let us remark that while studies using MDS are not reported for procaine, the penetrations of lidocaine and tetracaine do match the results observed in previous works [42,56].

3.2. Interacting energies

In Fig. 3 we depict snapshots of representative Coulomb and dispersion energy profiles produced by the interaction of each drugs with the membrane at a given time. It is important to remark that these are not energy landscapes, but only snapshots to show how the drugs interact with the lipids, i.e. to assess the relevance of the Coulomb and van der Waals contributions. In other words, we are not interested in measuring the free energy of the drug-membrane system at each penetration, rather, we would like to obtain a graphic notion about the interaction energy a drug molecule produces with the lipids close to it. Fig. 3 illustrates very nicely that all the anesthetics have a van der Waals interaction stronger than Coulomb, and lipids outside the action zone (of a particular drug molecule) do not feel their presence (the membrane remains unperturbed). This, of course, makes us understand why there is an effective dose to reach a whole effect (fluidization) in the membrane. Average interaction energies (during the last 80 ns of the simulation and the 10 drugs) are given in Table 1. In Fig. 4 we depict a middle slice of the membrane where the structural effects produced by each drug are sharply observed.

An important parameter seems to emerge from the energy values given in Table 1: if the ratio between Lennard-Jones and Coulomb energies (here we call it γ) is larger than one, the drug has a large probability to diffuse into the membrane. Polar molecules, for example caffeine, have much greater Coulomb energies and therefore γ is less than one [57]. This means that they cannot enter into the membrane.

Nevertheless, the profiles shown in Fig. 3 (or the values of γ in Table 1) are not sufficient data to understand why, for example, tetracaine produces more disorder than lidocaine as observed in Fig. 4. Then, we use the number of freely rotating bonds of the drugs as a second parameter to understand the observed disorder (see Table 1). Indeed, although tetracaine has a bit less van der Waals interaction (compared to lidocaine, see Fig. 3), is less rigid and therefore, due to the thermal energy, produces more disorder once it diffuses into the membrane.

Furthermore, although the slice depicted in Fig. 4 (extracted from our MD simulations) is useful to visually appreciate the disorder of the membranes induced by the drugs, we still need a more quantitative way to measure how the structural properties of the bilayer are modified by them. So we need to evaluate configurational entropies and an order parameter.

3.3. Configurational entropy

A sample of 22 DPPC molecules were taken to calculate the entropy of the membrane; 11 molecules per layer (upper and lower). The entire molecular structures were taken into consideration. The last 5000 configurations (out of the 50,000 possible) were used as states to evaluate the final Schlitter's entropy value, which is provided by a subroutine built in GROMACS. As seen in Fig. 5, the increasing values on the Schlitter entropies reveal an
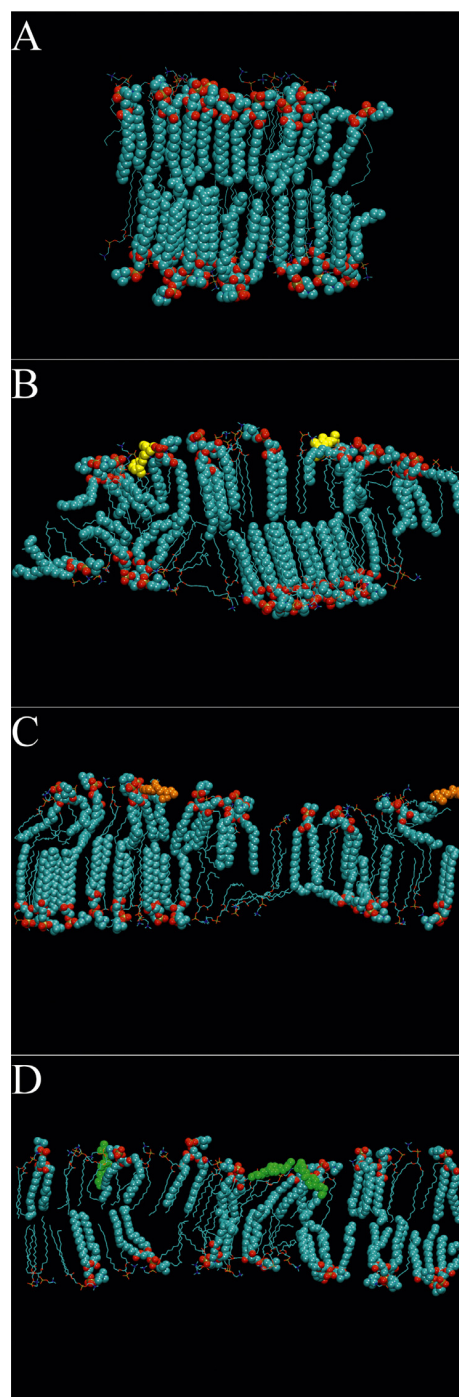

Fig. 4. (A) Middle slice of the unperturbed DPPC membrane; (B) the membrane under the influence of lidocaine; (C) the membrane under the influence of procaine; (D) the membrane under the influence of tetracaine. Comparing (A) with (B–D) the effect of the drugs is clearly noticed.

interesting pattern. The lowest value is for the control membrane and higher ones, at least 10% more, for the case when anesthetics are inside. The obtained results indicate that these non-polar drugs cause the destabilization (fluidization) of the membranes. In order to verify our findings, we evaluate Schlitter's entropy for a control membrane (with no drugs) at a higher temperature (44 °C), where a DPPC bilayer is in the fluidized state. Fig. 5 includes the entropy
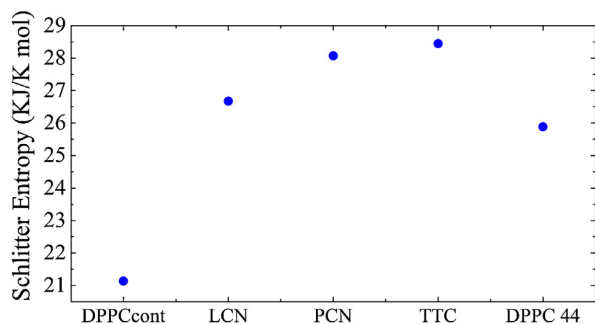
Fig. 5. Schlitter's configurational entropy for two pure membranes (at 37 and 44 °C) and for the membranes under the influence of lidocaine, procaine and tetracaine. The statistical error for each measurement is 0.5 J/kmol.
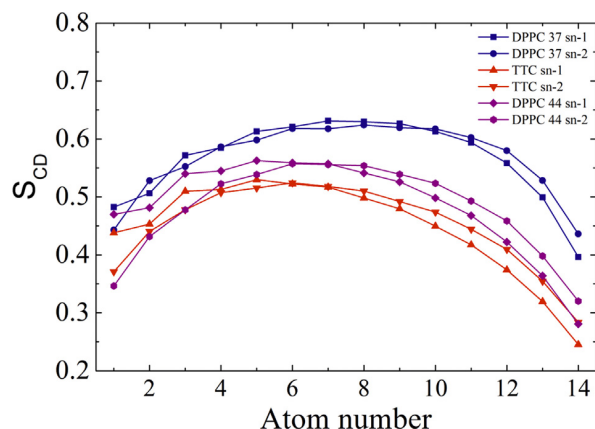

Fig. 6. The orientational order parameters for the DPPC control membrane (at 37 and 44 °C) and DPPC–tetracaine. Each carbon tail is represented by sn-1 and sn-2.

for this case, where one can notice that such value is similar to the one obtained under the influence of lidocaine.

Finally, in Fig. 6 we show S_{CD} for the control DPPC membranes (at 37 and 44 °C) and DPPC doped with tetracaine. It is clear that the order of the membrane diminishes in the presence of the anesthetic, offering further evidence on how anesthetics fluidize the bilayer. These parameters are also plotted for the pure membrane at a higher temperature (44 °C), noticing that temperature gives rise to fluidization too.

4. Conclusions

Despite the overwhelming endorsement of protein mechanisms to explain how anesthetics act, it is difficult to discern whether ion channel modulation by anesthetics is caused indirectly by changes in membrane structure or directly by binding to protein sites. The crucial role of lipids in neural structure and function demands that we maintain them as viable subjects of further research to elucidate the general anesthetic mechanism [58].

For such endeavour, in this article we employed Molecular Dynamic Simulations to investigate the interaction of three cationic amphiphilic drugs on a pure lipid membrane. Although it has been known for a long time that anesthetics fluidize lipid membranes, energetic and entropic details about how the former interact with the latter are still unknown. Thus, for the first time energy profiles and configurational entropies were calculated to provide a quantitative measure of the structural changes of the membrane upon the addition of the drugs. Our results may shed light on an important aspect not well understood in pharmacology: what is the effect local anesthetics have on the lipidic structures of plasma membranes. Although the lipid-based hypothesis of anesthetic action seems to be at odds with a wealth of experimental observations, quantifying the lipid disorder produced by an anesthetic on a model bilayer is important to understand its overall influence in real situations (for instance, around or inside lipid rafts).

References

[1] J.F. Butterworth, G.R. Strichartz, Molecular mechanisms of local anesthesia: a review, Anesthesiology 72 (1990) 711–734.
[2] B. Nilius, K. Benndorf, F. Markwardt, Effects of lidocaine on single cardiac sodium-channels, J. Mol. Cell. Cardiol. 19 (1987) 865–874.
[3] T. Weiser, Comparison of the effect of four Na$^+$ channel analgesics on TTX-resistant Na$^+$ currents in rat sensory neurons recombinant Mav 1.2 channels, Neurosci. Lett. 395 (2006) 179–184.
[4] T. Narahashi, D.T. Frazier, M. Yamada, Cationic forms of local anesthetics block action potentials from inside nerve membrane, Nature 223 (1969) 748–749.
[5] N.P. Franks, W.R. Lieb, Molecular and cellular mechanisms of general anesthesia, Nature 367 (1994) 607–614.
[6] M.F. Sheets, D.A. Hanck, Molecular action of lidocaine on the voltage sensors of sodium channels, J. Gen. Physiol. 121 (2003) 163–175.
[7] G.M. Lipkind, H.A. Fozzard, Molecular modeling of local anesthetic drug binding by voltage-gated sodium channels, Mol. Pharmacol. 68 (2005) 1611–1622.
[8] D.S. Ragdale, J.C. McPhee, T. Scheuer, W.A. Catterall, Molecular determinants of state-dependent block of Na$^+$ channels by local anesthetics, Science 265 (1994) 1724–1728.
[9] H.L. Li, A. Galue, L. Meadows, D.S. Ragsdale, A molecular basis for the different local anesthetic affinities of resting versus open and inactivated states of the sodium channel, Mol. Pharmacol. 55 (1999) 134–141.
[10] N.J. Linford, A.R. Cantrell, Y. Qu, T. Scheuer, W.A. Catterall, Interaction of batrachotoxin with the local anesthetic receptor site in transmembrane segment IVS6 of the voltage-gated sodium channel, Proc. Natl. Acad. Sci. U.S.A. 95 (1998) 13947–13952.
[11] R.S. Cantor, The influence of membrane lateral pressures on simple geometric models of protein conformational equilibria, Chem. Phys. Lipids 101 (1999) 45–56.
[12] I. Ueda, T. Yoshida, Hydration of lipid membranes and the action mechanisms of anesthetics and alcohols, Chem. Phys. Lipids 101 (1999) 65–79.
[13] Y. Boulanger, S. Schreier, I.C. Smith, Molecular details of anesthetic–lipid interaction as seen by deuterium and phosphorus-31 nuclear magnetic resonance, Biochem. J. 20 (1981) 6824–6830.
[14] M. Auger, I.C. Smith, H.H. Mantsch, P.T. Wong, High-pressure infrared study of phosphatidylserine bilayers and their interactions with the local anesthetic tetracaine, Biochem. J. 29 (1990) 2008–2015.
[15] L.M. Pinto, D.K. Yokaichiya, L.F. Fraceto, E. de Paula, Interaction of benzocaine with model membranes, Biophys. Chem. 87 (2000) 213–223.
[16] K.H. Meyer, Contribution to the theory of narcosis, Trans. Faraday Soc. 33 (1937) 1060–1068.
[17] C.E. Overton, in: R. Lipnick (Ed.), Studien über die Narkose, Verlag Gustav Fischer, Jena, Germany, 1901 (English translation: Studies of Narcosis, Chapman and Hall, 1991).
[18] D. Leckband, J. Israelachvili, Intermolecular forces in biology, Q. Rev. Biophys. 34 (2001) 105–267.
[19] D. Papahadjopoulos, K. Jacobson, G. Poste, G. Shepherd, Effect of local anesthetics on membrane properties. I. Changes in the fluidity of phospholipid bilayer, Biochim. Biophys. Acta 394 (1975) 504–519.
[20] I. Vorobyov, W.F.D. Bennett, D.P. Tieleman, T.W. Allen, S. Noskov, The role of atomic polarization in the thermodynamics of chloroform partitioning to lipid bilayers, J. Chem. Theory Comput. 8 (2) (2012) 618–628.
[21] J.P.M. Jämbeck, A.P. Lyubartsev, Implicit inclusion of atomic polarization in modeling of partitioning between water and lipid bilayers, Phys. Chem. Chem. Phys. 15 (13) (2013) 4677–4686.
[22] J.P.M. Jämbeck, F. Mocci, A.P. Lyubartsev, A. Laaksonen, Partial atomic charges and their impact on the free energy of solvation, J. Comput. Chem. 34 (3) (2013) 187–197.
[23] A. Pohorille, P. Cieplak, M.A. Wilson, Interactions of anesthetics with the membrane–water interface, Chem. Phys. 204 (2–3) (1996) 337–345.
[24] R.G. Eckenhoff, Promiscuous ligands and attractive cavities: how do the inhaled anesthetics work? Mol. Interv. 1 (5) (2011) 258–268.
[25] M. Pickholz, L. Saiz, M.L. Klein, Concentration effects of volatile anesthetics on the properties of model membranes: a coarse-grain approach, Biophys. J. 88 (2005) 1524–1534.
[26] G. Brannigana, D.N. LeBard, J. Hénin, R.G. Eckenhoff, M.L. Klein, Multiple binding sites for the general anesthetic isoflurane identified in the nicotinic

acetylcholine receptor transmembrane domain, Proc. Natl. Acad. Sci. U.S.A. 107 (2010) 14122–14127.

[27] T. Heimburg, A.D. Jackson, On soliton propagation in biomembranes and nerves, Proc. Natl. Acad. Sci. U.S.A. 102 (2005) 9790–9795.

[28] T. Heimburg, A.D. Jackson, On the action potential as a propagating density pulse and the role of anesthetics, Biophys. Rev. Lett. 2 (2007) 57–78.

[29] G.R. Strichartz, V. Sanchez, G.R. Arthur, R. Chafetz, D. Martin, Fundamental properties of local anesthetics. II. Measured octanol:buffer partition coefficients and pK, values of clinically used drugs, Anesth. Analg. 71 (1990) 158–170.

[30] R.W. Pastor, Computer simulations of lipid bilayers, Curr. Opin. Struct. Biol. 4 (1994) 486–492.

[31] D.P. Tieleman, H.J.C. Berendsen, Molecular dynamics simulations of a fully hydrated dipalmitoylphosphatidylcholine bilayer with different macroscopic boundary conditions and parameters, J. Chem. Phys. 105 (1996) 4871–44880.

[32] O. Berger, O. Edholm, F. Jähnig, Molecular dynamics simulations of a fluid bilayer of dipalmitoylphosphatidylcholine at full hydration, constant pressure and constant temperature, Biophys. J. 72 (1997) 2002–2013.

[33] H.L. Scott, Modeling the lipid component of membranes, Curr. Opin. Struct. Biol. 12 (2002) 495–502.

[34] F.L. Lopes, S.O. Nielsen, M.L. Klein, Hydrogen bonding structure and dynamics of water at the dipalmitoylphosphatidylcholine lipid bilayer surface from a molecular dynamics simulation, J. Phys. Chem. B 108 (2004) 6603–6610.

[35] C.J. Högberg, A.P. Lyubartsev, A molecular dynamics investigation of the influence of hydration and temperature on structural and dynamical properties of a dimyristoylphosphatidylcholine bilayer, J. Phys. Chem. B 110 (2006) 14326–14336.

[36] E. Falck, M. Patra, M. Karttunen, M.T. Hyvonen, I. Vattulainen, Lessons of slicing membranes: interplay of packing, free area, and lateral diffusion in phospholipid/cholesterol bilayers, Biophys. J. 87 (2004) 1076–1091.

[37] M. Patra, E. Salonen, E. Terama, I. Vattulainen, R. Faller, B.W. Lee, J. Holopainen, M. Karttunen, Under the influence of alcohol: the effect of ethanol and methanol on lipid bilayers, Biophys. J. 90 (2006) 1121–1135.

[38] U.R. Pedersen, G.H. Peters, P. Westh, Molecular packing in 1-hexanol-DMPC bilayers studied by molecular dynamics simulations, Biophys. Chem. 125 (2007) 104–111.

[39] E. Yamamoto, T. Akimoto, H. Shimizu, Y. Hirano, M. Yasui, K. Yasuoka, Diffusive nature of xenon anesthetic changes properties of a lipid bilayer: molecular dynamics simulations, J. Phys. Chem. B 116 (2012) 8989–8995.

[40] G.A. Jamieson, D.M. Robinson, Mammalian Cell Membranes, vol. 2, Butterworths, London, 1977.

[41] J. Krüeger, W.B. Fischer, Exploring the Conformational Space of VPU from HIV-1: a versatile adaptable protein, J. Comput. Chem. 29 (2008) 2416–2424.

[42] C.J. Högberg, A. Maliniak, A.P. Lyubartsev, Dynamical and structural properties of charged and uncharged lidocaine in a lipid bilayer, Biophys. Chem. 125 (2007) 416–424.

[43] D.M. Van Aalten, R. Bywater, J.B. Findlay, M. Hendlich, R.W. Hooft, G. Vriend, PRODRG, a program for generating molecular topologies and unique molecular descriptors from coordinates of small molecules, J. Comput. Aided Mol. Des. 10 (1996) 255–262.

[44] C.J. Högberg, A.P. Lyubartsev, Effect of local anesthetic lidocaine on electrostatic properties of a lipid bilayer, Biophys. J. 94 (2008) 525–531.

[45] E.H. Mojumdar, A.P. Lyubartsev, Molecular dynamics simulations of local anesthetic articaine in a lipid bilayer, Biophys. Chem. 153 (2010) 27–35.

[46] V. Zoete, M.A. Cuendet, A. Grosdidier, O. Michielin, SwissParam: a fast force field generation tool for small organic molecules, J. Comput. Chem. 11 (2011) 2359–2368.

[47] C. Oostenbrink, T.A. Soares, N.F. van der Vegt, W.F. van Gunsteren, Validation of the 53A6 GROMOS force field, Eur. Biophys. J. 34 (2005) 273–284.

[48] B. Hess, H. Bekker, H.J.C. Berendsen, J. Fraaije, LINCS: a linear constraint solver for molecular simulations, J. Comput. Chem. 18 (1997) 1463–1472.

[49] D.J. Evans, B.L. Holian, The Nose–Hoover thermostat, J. Chem. Phys. 83 (1985) 4069–4074.

[50] M. Parrinello, A. Rahman, Polymorphic transitions in single crystals: a new molecular dynamics method, J. Appl. Phys. 52 (1981) 7182–7190.

[51] C. Neale, W.F.D. Bennett, D.P. Tieleman, R. Pomes, Statistical convergence of equilibrium properties in simulations of molecular solutes embedded in lipid bilayers, J. Chem. Theory Comput. 7 (2011) 4175–4188.

[52] M. Paloncyova, K. Berka, M. Otyepka, Convergence of free energy profile of coumarin in lipid bilayer, J. Chem. Theory Comput. 8 (2012) 1200–1211.

[53] B. Hess, C. Kutzner, D. Van der Spoel, E. Lindahl, Gromacs 4: algorithms for highly efficient, load-balanced, and scalable molecular simulation, J. Chem. Theory Comput. 4 (2008) 435–447.

[54] J. Schlitter, Estimation of absolute and relative entropies of macromolecules using the covariance matrix, Chem. Phys. Lett. 215 (1993) 617–621.

[55] H. Schafer, A.E. Mark, W.F. van Gunsteren, Absolute entropies from molecular dynamics simulation trajectories, J. Chem. Phys. 113 (2000) 7809–7817.

[56] R.C. Bernardi, D.E.B. Gomes, R. Gobato, C.A. Taft, A.T. Ota, P.G. Pascutti, Molecular dynamics study of biomembrane/local anesthetics interactions, Mol. Phys. 107 (2009) 1437–1443.

[57] F.J. Sierra-Valdez, L.S. Forero-Quintero, P.A. Zapata-Morin, A. Miguel Costas, J.C. Chavez-Reyes, Ruiz-Suarez, The influence of non polar and polar molecules in mouse motile cells membranes and pure lipid bilayers, PLOS ONE 8 (4) (2013) e59364, http://dx.doi.org/10.1371/journal.pone.0059364.

[58] G.A. Mashour, S.A. Forman, J.A. Campagna, Mechanisms of general anesthesia: from molecules to mind, Best Pract. Res. Clin. Anaesthesiol. 19 (2005) 349–364.